ResearchGate

See discussions, stats, and author profiles for this publication at: https://www.researchgate.net/publication/320779557

Locomotion Control of Three Dimensional Passive-Foot Biped Robot Based on Whole Body Operational Space Framework

Conference Paper · December 2017

DOI: 10.1109/ROBIO.2017.8324642

CITATION
1

READS
335

5 authors, including:

Jianwen Luo
Stanford University
9 PUBLICATIONS **9** CITATIONS
SEE PROFILE

Ye Zhao
Harvard University
32 PUBLICATIONS **618** CITATIONS
SEE PROFILE

Donghyun Kim
University of Texas at Austin
19 PUBLICATIONS **45** CITATIONS
SEE PROFILE

Luis Sentis
University of Texas at Austin
77 PUBLICATIONS **1,848** CITATIONS
SEE PROFILE

Some of the authors of this publication are also working on these related projects:

Trikey Robot View project

Valkyrie View project

All content following this page was uploaded by Jianwen Luo on 01 November 2017.

The user has requested enhancement of the downloaded file.

Locomotion Control of Three Dimensional Passive-Foot Biped Robot Based on Whole Body Operational Space Framework

Jianwen Luo[1], Ye Zhao[2], Donghyun Kim[3], Oussama Khatib[4], Luis Sentis[5]

***Abstract*— In this paper, whole body operational space (WBOS) framework for three dimensional passive-foot biped robot is presented. The stability of WBOS controller is analyzed and a foot placement planner is proposed. In many cases, WBOS controller generates torque commands to execute the trajectories planned by high-level planners every control loop. The planners find the trajectories by watching the behaviors of longer time horizon. Instead, our planner updates a step location every control loop by watching the center-of-mass (CoM) state to achieve robust balancing. The robustness is also enhanced because contact events vary the stance leg switching time from the given nominal step frequency. Via this new foot placement planner, the locomotion's robustness to unknown terrains is improved. Dynamically stable walking on flat and unknown terrains, and push recovery are tested in real-time dynamic simulation.**

I. INTRODUCTION

Balancing biped robot is about stabilizing CoM dynamics of whole body and posture of it, which is a low dimensional task [1]. However, biped robot is a highly nonlinear system whose high dimensional joint space is difficult to analyze directly. Therefore, to simplify the whole body dynamics, point mass models such as inverted pendulum are proposed and motion planners of these simplified models are designed in the high level of the hierarchical control framework. In the low level whole body controller (WBC) solves joint torques to execute the trajectory planned by high level motion planner [2].

Various point mass models have been proposed for the high level motion planner. A widely-studied one is Linear Inverted Pendulum Model (LIPM) [3]–[5], of which the CoM height is constant and the dynamics is linearized. LIPM opens many methods in which classic control theory for linear system could be applied. Based on LIPM dynamics, instantaneous capture point (ICP) is derived [6]. One important property of ICP is that the velocity at the top of ICP is zero. This was utilized to realize one-step stop and push recovery [7], [8]. However, LIPM ignores contact impact and assumes the angular momentum to be zero. And usually the step timing is fixed. Divergent component of motion (DCM) is another well-received method that extends ICP to three dimensional situation. Similar to ICP, the swing time of DCM method needs to be preplanned [9]–[11]. Another well-received model is spring-loaded inverted pendulum (SLIP) [12], [13]. SLIP inherently achieves compliance by using an elastic element in the leg. The spring leg stores the energy during stance phase. This locomotion compliance is critical for walking efficiency and contact safety. For instance, ATRIAS is a three dimensional passive-foot biped robot which embodies a three dimensional spring-mass model and can walk very efficiently [14]–[16]. Prismatic inverted pendulum model(PIPM) is another practical point mass model which has been successfully implemented in three dimensional point-foot biped robot Hume [17], [18]. PIPM considers the CoM's position variance in vertical direction and plans CoM motion in horizontal plane.

At low level WBC normally computes joint torques to comply with the planned CoM dynamics and sends desired torques or positions to joint actuators. WBC models biped robots as rigid body dynamics with floating base and physical constraints [19]. The dynamics are formulated to accomplish multiple tasks in operational space through controlling torques in joint space. And contacts are modeled as constraints in an optimization problem, which can be solved through Jacobian-transpose methods [20], [21] or projection-based techniques such as operational space methods [22]. A main advantage of projection-based techniques is that the time-consuming optimization is not needed. An alternative way is the quadratic programming [23]–[25], which allows for inequality constraints but suffers slower computations. Operational space control is applied to humanoid robots, which can be modeled as a rigid multi-body system with a floating base and in contact with environments including the ground [19]. Various related works are influenced by this framework [26]–[28].

In this paper, a strategy which integrates the motion planner into WBC is presented for locomotion control of a three dimensional passive-foot biped robot. The key to balancing a biped robot is controlling the horizontal motion of the CoM [1]. For a highly under-actuated system such as passive-foot biped robot, the CoM motion in horizontal plane could be bounded through continuously updating foot placements. Therefore, this study proposes a foot placement planner, which is analogous to the ideas in [29], [30], as a motion planner to update the foot placements. This strategy is different from the traditional walking control strategies based on ZMP [31]. The contributions of this study lie in twofold: First, the foot placement planner is not explicitly

*This work was not supported by any organization

[1]Jianwen Luo is with State Key Laboratory of Robotics and System, Harbin Institute of Technology, Harbin, 15000, CHINA luojianwen1123@gmail.com

[2]Ye Zhao is with Agile Robotics Lab, Harvard University, Cambridge, MA 02138, USA yez@seas.harvard.edu

[4]Oussama Khatib is with Stanford Robotics Lab, Stanford University, Stanford, CA 94305, USA ok@cs.stanford.edu

[3]Donghyun Kim and [5]Luis Sentis is with Human Centered Robotics Group, University of Texas in Austin, Austin, TX 78712, USA dk6587@utexas.edu, lsentis@austin.utexas.edu

based on point mass model. In the task of WBOS framework, the desired CoM height is set to be constant whereas the acceleration is not constrained to be zero; Second, nominal step frequency is predefined, however, considering the unforeseen contact impact due to the unknown terrains, the dynamics model switches based on contact events and thus the swing time is adjustable. Frequent updating of the foot landing position naturally improves the robustness of the foot placement to terrain uncertainty. Real-time simulations demonstrate that the robot's CoM can be maintained within a stable bounded region.

The paper is organized as follows. Section II introduces the simulated robot configuration. Section III presents the WBOS framework. Section IV proposes the walking task design and foot placement planner. Simulation results are shown in Section V. And this line of research is concluded in Section VI.

II. Configuration of the Passive-Foot Biped Robot

The three dimensional passive-foot biped robot in this study has six actuated degree-of-freedoms (DoFs) as shown in Fig. 1. The robot model originates from the real robot in [32]. As a modification, the actuated ankles are removed and replaced with passive feet. The robot has a torso, two thighs, two shanks and two passive feet. There are roll and pitch joints on hips, pitch joints on knees and pure passive pitch joints on ankles. The passive feet are equipped under the ankles to provide resistant friction torque to oppose the yaw rotational disturbance from the whole body motion. The sagittal x-z plane is annotated in Fig. 1.

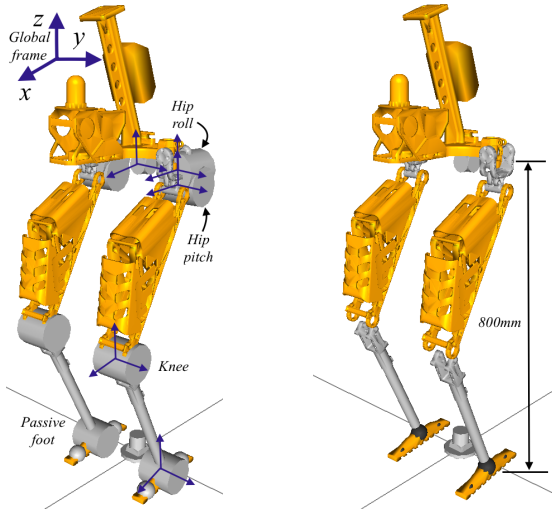

Fig. 1. Three dimensional passive-foot biped robot. The left figure shows the coordinate definition and the right figure is an overview of the biped robot

The base frame is selected as the free-floating torso. Six virtual joints (three prismatic joints and three revolute joints) are connected from the base frame to the ground. Therefore, the total DoFs of the robot system is twelve, including six actuated joints and six virtual joints.

III. Whole Body Operational Space Framework

In this section, the whole body operational space (WBOS) framework is briefly introduced. According to [19], the WBOS dynamics with contact constraints are given as below.

$$A\ddot{q} + N_c^T(b+g) + J_c^T \Lambda_c \dot{J}_c \dot{q} = (SN_c)^T \tau \tag{1}$$

where $q \in \mathbb{R}^{(n+6)}$ is generalized coordinates. n is the number of actuated degrees-of-freedom (DOFs). A is mass inertia matrix, b is centrifugal and Coriolis vector and g is gravity vector. J_c is contact jacobian (left or right foot). For single stance in our robot model, $J_c \in \mathbb{R}^{3\times 12}$. S is the selection matrix. $\tau \in \mathbb{R}^n$ is the actuated torque. Null space projection $N_c = I - \overline{J}_c J_c$. The contact constraints are $\ddot{x}_c = J_c\ddot{q} + \dot{J}_c\dot{q} = 0$. x_c is the contact point on the foot.

Since the walking process is highly dynamic, the double stance phase is quite short and almost ignorable. We assume the double stance to be instantaneous. The whole dynamics are switched between left and right single stances. In task space, the generalized force is given in Eq. (2).

$$F_{\text{task}} = \Lambda^*_{\text{task}} u_{\text{task}} + \mu^*_{\text{task}} + p^*_{\text{task}} \tag{2}$$

where F_{task} is the generalized force in task space. Λ^*_{task} is kinetic energy matrix in task space. u_{task}, μ^*_{task} and p^*_{task} are task space acceleration, centrifugal and Coriolis force, and gravity force, respectively (see Eq. 3).

$$\begin{cases} \Lambda^*_{\text{task}} = (J^*_{\text{task}} \Phi J^{*T}_{\text{task}})^{-1}, \\ \mu^*_{\text{task}} = \Lambda^*_{\text{task}} J^*_{\text{task}} \Phi b - \Lambda^*_{\text{task}} \dot{J}^*_{\text{task}} \dot{q}, \\ p^*_{\text{task}} = \Lambda^*_{\text{task}} J^*_{\text{task}} \Phi g \end{cases} \tag{3}$$

where $\Phi = (SN_c)A^{-1}(SN_c)^T$ is the constrained projection of A^{-1}. $J^*_{\text{task}} = J_{\text{task}}\overline{(SN_c)} \in \mathbb{R}^{n_{\text{task}}\times 6}$. n_{task} is the number of tasks. $\overline{(SN_c)}$ is the support consistent generalized inverse of (SN_c). In general, the knee is never stretched straight in walking, thus singularity of the Jacobian does not need to be considered. Within this task space dynamics framework, τ is determined by $\tau = J^{*T}_{\text{task}} F_{\text{task}}$. In next section, F_{task} for multiple walking tasks is designed.

IV. Stable Walking Strategy

A. Walking tasks and dynamics control

Walking tasks include the center-of-mass (CoM) position, the body posture and swing foot. CoM task has three degree-of-freedoms (DoFs) (x, y and z position), posture task includes three DoFs (pitch, roll and yaw angles of the torso) and swing point foot has three DoFs ($x_{\text{foot}}, y_{\text{foot}}$ and z_{foot}). To control all the tasks, at least nine actuated DoFs are required. Since the biped robot studied only has six actuated DoFs, the yaw angle and the CoM motion in x and y axis are not controlled. So the task acceleration is designed as $u_{\text{walking}} = [\ddot{z}_{\text{CoM}}, \ddot{\theta}_{\text{pitch}}, \ddot{\theta}_{\text{roll}}, \ddot{x}_{\text{foot}}, \ddot{y}_{\text{foot}}, \ddot{z}_{\text{foot}}]^T$. The control architecture is depicted in Fig. 2. The aggregate walking task jabobian is given as below,

$$J_{\text{walking}} = \begin{bmatrix} J_{z_{\text{CoM}}} \\ J_{\text{posture}} \\ J_{\text{foot}} \end{bmatrix} \tag{4}$$

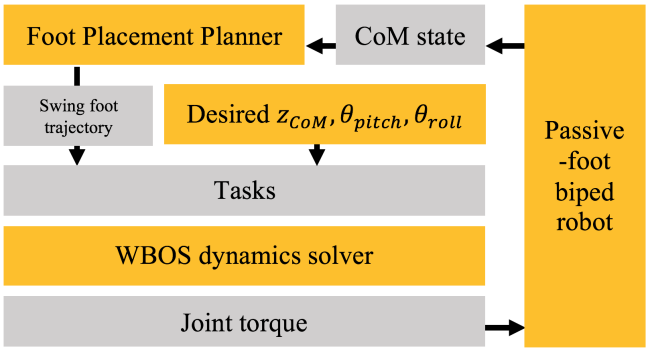

Fig. 2. WBOS-based Dynamics Control Architecture.

where $J_{z_{\text{CoM}}} \in \mathbb{R}^{1\times 12}$ is the jacobian for CoM in z axis, $J_{\text{posture}} \in \mathbb{R}^{2\times 12}$ is for pitch and roll angles of torso, and $J_{\text{foot}} \in \mathbb{R}^{3\times 12}$ is for spatial position of swing foot (either left or right foot). Based on the WBOS framework in Eq. (1), the torques are computed by Eq. (5).

$$\tau = J^{*T}_{\text{waking}}(\Lambda^{*}_{\text{walking}} u_{\text{walking}} + \mu^{*}_{\text{walking}} + p^{*}_{\text{walking}}) \tag{5}$$

where $J^{*}_{\text{waking}} = J_{\text{waking}}\overline{(SN_c)} \in \mathbb{R}^{6\times 12}$. In this walking task a PD controller is plugged in Eq. (5) and the WBOS controller for walking is designed as Eq. (6).

$$u_{\text{walking}} = k^{*}_{p}(r_{\text{des}} - r_{\text{act}}) + k^{*}_{d}(\dot{r}_{\text{des}} - \dot{r}_{\text{act}}) \tag{6}$$

where $r = [z_{\text{CoM}}, \theta_{\text{pitch}}, \theta_{\text{roll}}, x_{\text{foot}}, y_{\text{foot}}, z_{\text{foot}}]^T$. r_{des} and r_{act} are the desired and actual position of task vector r. k^{*}_{p} and k^{*}_{d} are PD gains respectively. In this study, the desired z_{CoM}, θ_{pitch} and θ_{roll} are set to be constants. The desired x_{foot}, y_{foot} and z_{foot} are designed in foot placement planner.

B. Stability analysis

For the WBOS controller in Eq. (6), $u_{\text{walking}} = \ddot{r}_{\text{act}}$. Define the task tracking error as

$$e = r_{\text{des}} - r_{\text{act}} \tag{7}$$

Then $\ddot{e} = \ddot{r}_{\text{des}} - \ddot{r}_{\text{act}}$. $\ddot{r}_{\text{des}}$ is set to be zero. As such, Eq. (6) can be rewritten in Eq. (8),

$$\ddot{e} + k^{*}_{d}\dot{e} + k^{*}_{p}e = 0 \tag{8}$$

Eq. (8) represents second-order exponentially stable error dynamics and thus the WBOS controller is guaranteed to be asymptotically stable.

The system states' jump comes from impact dynamics including foot-ground contact impact or unexpected external disturbances. The contact model can be described by Eq. (9).

$$\dot{q}^{+} = \dot{q}^{-} - \Delta_{\varepsilon}(\dot{q}^{-}, q^{-}) \tag{9}$$

where $+$ and $-$ denote before and after contact. $\dot{q}$ is joint velocity. The restitution ε is set to be zero. The system energy $E = \frac{1}{2}\dot{q}^{T}A\dot{q}$ is dissipative during the impact. Therefore, $E^{+} = \frac{1}{2}\dot{q}^{+T}A\dot{q}^{+} \leq E^{-} = \frac{1}{2}\dot{q}^{-T}A\dot{q}^{-}$.

$$\|\dot{q}^{+}\| = \|\dot{q}^{-} - \Delta_{\varepsilon}(\dot{q}^{-}, q^{-})\| \leq \|\dot{q}^{-}\| \tag{10}$$

In this study state jump can be assumed to be bounded so that the joint velocity is finite after the impact.

C. Foot placement planner

Foot placement planner is designed to control the CoM dynamics in horizontal plane. In the WBOS controller z_{CoM} is controlled as a task while x_{CoM} and y_{CoM} are not directly controlled as tasks. Therefore, the x_{CoM} and y_{CoM} states evolute by following its natural dynamics. Foot placement planner is to provide the desired landing point on the ground so that x_{CoM} and y_{CoM} are kept from diverging excessively from the support point. The concept of stable walking of the biped robot could be defined as that the CoM states $[x_{\text{CoM}}, \dot{x}_{\text{CoM}}]^T$, $[y_{\text{CoM}}, \dot{y}_{\text{CoM}}]^T$ and $[z_{\text{CoM}}, \dot{z}_{\text{CoM}}]^T$ are controlled within a bounded ball-shape region in the phase space, respectively. The foot placement planner in this study is proposed as below,

$$\rho = \xi + \lambda\dot{\xi} \tag{11}$$

where $\rho = [x_{\text{foot}},\ y_{\text{foot}}]^T$ is the planned foot position. λ is a coefficient. $\xi = [x_{\text{CoM}},\ y_{\text{CoM}}]^T$ is the CoM position in horizontal plane. Eq. (11) is the same as [29], [30] in form. The reachable space of ρ is limited by,

$$\rho \in \Omega = \{[x_{\text{foot}},\ y_{\text{foot}}]^T \in \mathbb{R}^2 |\ \ ||r_{\text{foot}} - r_{\text{torso}}|| < l\} \tag{12}$$

where $r_{\text{foot}} = [x_{\text{foot}}, y_{\text{foot}}, z_{\text{foot}}]^T$. r_{torso} is the origin of torso's local frame. l is the maximum distance between torso and foot.

Ground reaction force (GRF) can be computed using joint torques and joint states as given in Eq. (13).

$$F_c = \bar{J}^{T}_{c}[S^{T}\tau - b - g] + \Lambda_c\dot{J}_c\dot{q} \tag{13}$$

where $\bar{J}_c = A^{-1}J^{T}_{c}\Lambda_c$ and the GRF $F_c = [F_{cx}, F_{cy}, F_{cz}]^T \in \mathbb{R}^3$. Within the WBOS framework, F_c is the function of q, $\dot{q}$, and τ. The generic CoM dynamics is given in Eq. (14)

$$\begin{bmatrix} F_{cxy} \\ F_{cz} \end{bmatrix} = m \begin{bmatrix} \ddot{\xi} \\ \ddot{z} + g \end{bmatrix} \tag{14}$$

where $F_{cxy} = [F_{cx},\ F_{cy}]^T$, m is the total mass of the robot and g is gravity. To analyze the stability of proposed foot placement planner, we take CoM dynamics in y direction for example. Ignoring the angular momentum, then we have,

$$\frac{F_{cy}}{F_{cz}} = \frac{(y - p_y)}{z} \tag{15}$$

where p_y is the supporting foot position. Combine Eq. (15) with Eq. (14), Eq. (16) can be obtained as below,

$$\ddot{y} = \frac{(g + \ddot{z})}{z}(y - p_y) \tag{16}$$

If within a short time span $\ddot{z}$ can be taken as a constant, and considering the CoM height is set to be constant in our walking tasks, then Eq. (16) is approximately linear and thus has an analytical solution as below,

$$y(t) = \frac{1}{2}(y_0 + \frac{\dot{y}_0}{\omega} - p_y)e^{\omega t} + \frac{1}{2}(y_0 - \frac{\dot{y}_0}{\omega} - p_y)e^{-\omega t} + p_y \tag{17}$$

where $\omega = \sqrt{\frac{g+\ddot{z}}{z}}$. y_0 and $\dot{y}_0$ are initial position and velocity of CoM. The first term in Eq. (17) is a divergent component.

Choose $p_y = y_0 + \dot{y}_0/\omega$, then as time t tends to infinity, $y(+\infty) = p_y$. In this case, the foot placement position is instantaneous capture point (ICP), on the top of which CoM will stop. However, within a stance phase the CoM dynamics in horizontal plane has finite time to diverge. As long as the CoM states are bounded within a desired region, dynamically stable walking can be achieved. Therefore, to control the CoM states within a bounded region, the coefficient of the first term in Eq. (17) is not necessary to be zero within a finite time span. Considering the variance of $\ddot{z}$ and z within one stance phase, $\omega = \omega(t),\ t \in [t_{\text{initial}}, t_{\text{final}}]$. Let $\omega_{\min} = \min[\omega(t)],\ t \in [t_{\text{initial}}, t_{\text{final}}]$, then a certain p always exists such that

$$p_{\text{ymax}} = y_0 + \frac{\dot{y}_0}{\omega_{\min}} > y_0 + \frac{\dot{y}_0}{\omega} \tag{18}$$

When CoM diverges from the support point, $\dot{y}_0 > 0$. Then Eq. (19) is always satisfied.

$$p_{\text{ymax}} = y_0 + \frac{\dot{y}_0}{\omega_{\min}} > y_0 - \frac{\dot{y}_0}{\omega} \tag{19}$$

Then from Eq. (17), we will have,

$$y(t) < p_{\text{ymax}},\ \ t \in [t_{\text{initial}}, +\infty] \tag{20}$$

This inequality can guarantee that even if there is divergent component in Eq. (17) due to the variance of $\ddot{z}$ and z, p_{ymax} can still strictly guarantee that CoM will never escape beyond p_{ymax}. Frequent stepping shortens phase time, which limits the divergence of CoM in horizontal plane and thus p_{ymax} is finite. In Eq. (11) we can choose a proper $\lambda = [\lambda_1, \lambda_2]^T = [1/\omega_1, 1/\omega_2]^T$ such that the planner is stable.

The desired foot landing position actually keeps updating during the entire swing process until the foot touches the ground. The trajectory of lifting foot z_{foot} is designed with a sine function $z_{\text{foot}} = \alpha sin(\omega_f t)$, where α is the peak height of the swinging foot and ω_f determines the nominal step frequency.

V. Simulation Results

In this simulation, The angular frequency ω_f of the lift foot is set to be 30 which corresponds to the nominal step frequency at around $2.38Hz$. The swing time is adjustable based on contact events. We do not control center-of-mass (CoM) of the robot through regulating ground reaction forces (GRFs). Instead, unexpected GRFs are treated as disturbances. The simulation results show that the proposed control method achieves dynamically stable stepping not only under push disturbance but also on unknown terrains.

A. Dynamically stable stepping

In real-time simulation dynamically stable stepping is tested on flat terrains without external disturbances. The foot placement planner adjusts the landing foot's position to adapt to contact disturbances from previous phase. During a time span of 300 seconds, the robot achieved around 717 steps without falling. The CoM dynamics are demonstrated in phase plane as shown in Fig. 3. It can be seen that the CoM states is bounded, and the CoM height is controlled

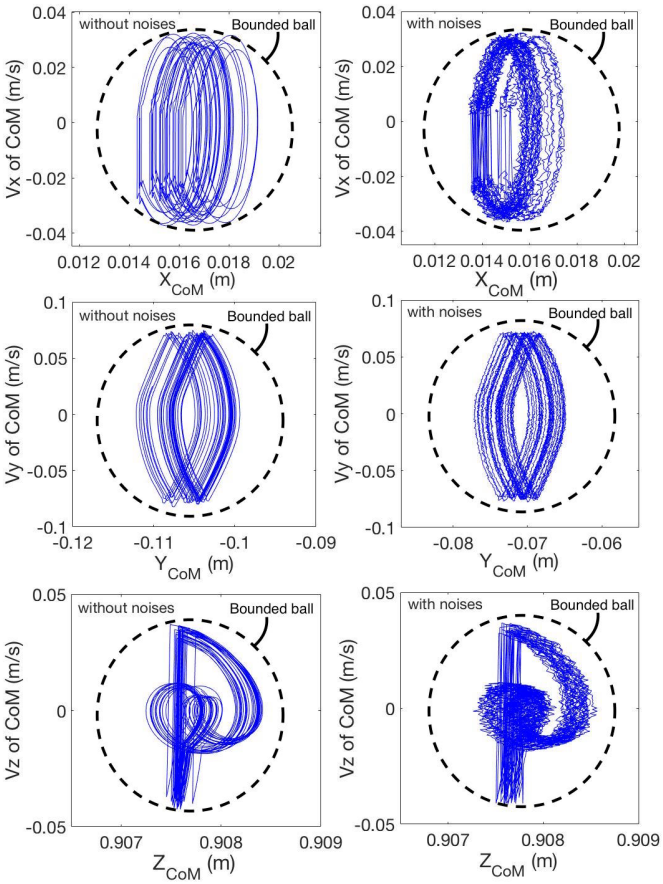

Fig. 3. Phase space in x, y and z direction. The vertical and horizontal axis are velocity and position of CoM respectively. The right column shows phase space with sensing noises included and the left column shows the phase space without sensing noises. Note that the scales of figures are different. z_{CoM} has almost no movement compared with the movement of x_{CoM} and y_{CoM}.

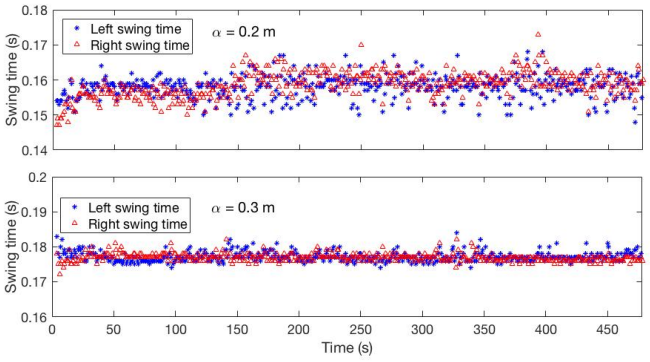

Fig. 4. The average swing time is $0.158s$ during 478 steps' simulation with peak height of swing foot α at $0.2m$. And the average swing time is $0.177s$ during 478 steps' simulation with peak height of swing foot α at $0.3m$

within the range [$0.9072m$, $0.9084m$] when desired CoM height is set to be $0.9m$. The fluctuation magnitude of the CoM height is around $1.2mm$, which means the CoM height is almost constant. However, this is achieved through WBOS framework instead of LIPM. Fig. 5 shows that $\dot{z}_{\text{CoM}}$ and $\ddot{z}_{\text{CoM}}$

are not zero, meaning that LIPM dynamics are not enforced in our control framework.

In this subsection random white noises are also added in the joint position and velocity to simulate the sensing noises. In this way the robustness of the controller proposed is tested in the simulation. The mean value of white noise is 0 and the variance is 1.0. The maximum value of the velocity noise is around 10% of the maximum value of joint velocity while the position noise is around 7%. Fig. 3 shows CoM states in phase space are bounded even if some sensing noises are included. This simulation results can be practical reference for real robot implementation.

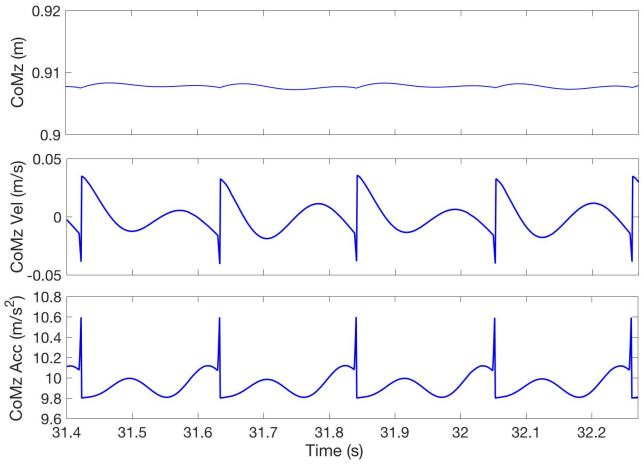

Fig. 5. The first subplot shows CoM position. The second and third subplot shows the CoM velocity and acceleration in z direction, respectively.

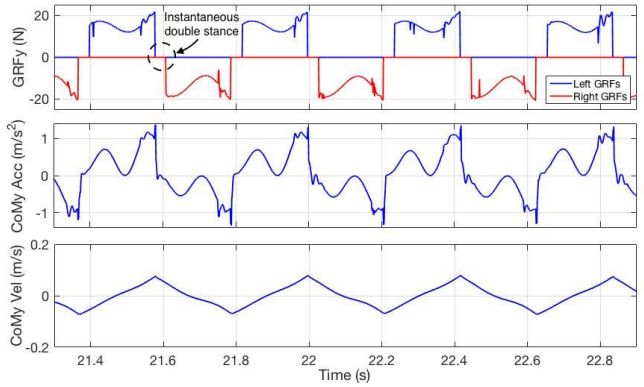

Fig. 6. The first subplot shows GRFy on left and right foot. The second and third subplot shows the CoM acceleration and velocity in y direction, respectively.

We test two different peak heights for the desired swing foot trajectory and measure the swing time (Fig. 4). The result shows that the average swing time takes longer due to higher swing height. We can also find that the swing time of each phase is not constant because in our foot placement planner swing time is adjusted based on contact events.

Fig. 6 depicts the GRFs and the CoM acceleration in y direction. The GRFs are computed using Eq. (13) and the peak value is about $20N$. It can also be found from the first subplot in Fig. 6 that there is an instantaneous transition between left and right stance. Since Eq. (13) is for single stance, we did not compute GRFs in double stance and internal force as in [17]. And thus in Fig. 6 double stance are not shown (taken as zero). It can also be seen from Fig. 6 that there are disturbance noises in CoM acceleration and GRFs whereas the velocity curve is relatively smooth. This is because the acceleration is integrated to obtain the velocity and therefore the disturbance noises from impact and uncontrolled transition are filtered.

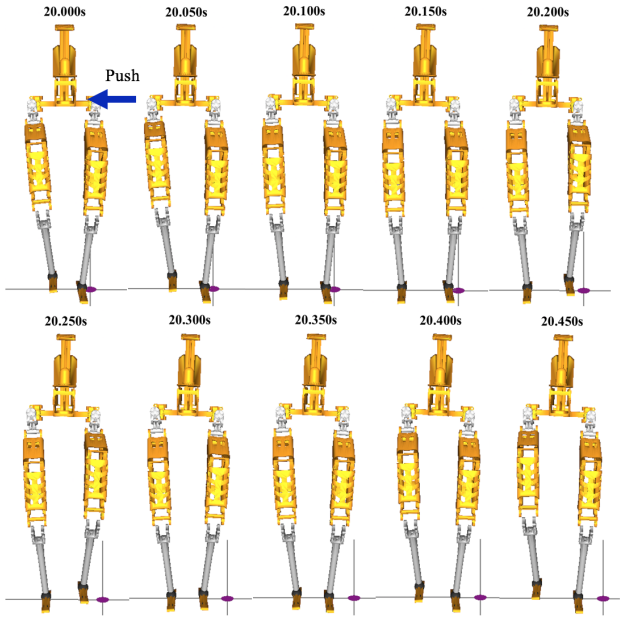

Fig. 7. Snapshots of push recovery. A sudden push is imposed on the torso at $20s$. The time step of the snapshots is $0.05s$.

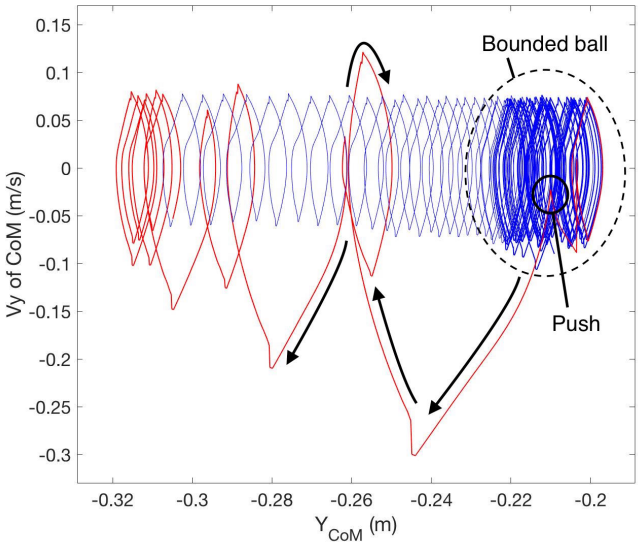

Fig. 8. The red line shows the evolution of the position and velocity of CoM in y direction after impulse is exerted on the robot. The CoM state moves in the direction of black arrows

B. Dynamically stable stepping with external disturbances

In this subsection we test the dynamically stepping under two kinds of external disturbances. One is from push while the other comes from unknown terrains.

Push recovery is demonstrated in Fig. 7. The push comes from an external impact on the right side of the torso at 20s, which suddenly changes the CoM velocity. The impact is 2100N and lasts for 0.002s, which is an impulse of 4.2 $N \cdot s$. In the simulation the total mass of the robot is around 30kg, of which the torso, hip, thigh and shank weigh 15.1kg, 2.3kg, 3.5kg and 1.1kg, respectively. The magnitude of this impact is larger than that from foot contact when comparing the velocity changes in Fig. 6 and Fig. 8. The robot adjusts the right leg to the larger-step side of the body to provide a re-planned foot support point. In Fig. 8 the red line depicts the evolution of CoM state after the impulse changes the robot's CoM velocity. After a few foot placement adjustments, the COM state establishes a bounded region in the phase plane.

The dynamically stable stepping on uneven terrain are tested as shown in Fig. 9. The robot has no prior knowledge of the terrains. When the right foot lands on an unexpected obstacle as the black box in Fig.9, the left foot starts to update a new foot placement. In the screen shots of Fig. 9, the robot steps on the obstacle twice and eventually keeps stepping on the flat ground. This simulation result shows the robot has robustness to the unknown terrains. Fig. 10 shows the swing time of each phase. The swing time is shortened when the foot lands ahead of time due to the obstacle. This can be seen in the first few points in Fig. 10. After the robot dose not touch the obstacle, the swing time tends to fall within a small range.

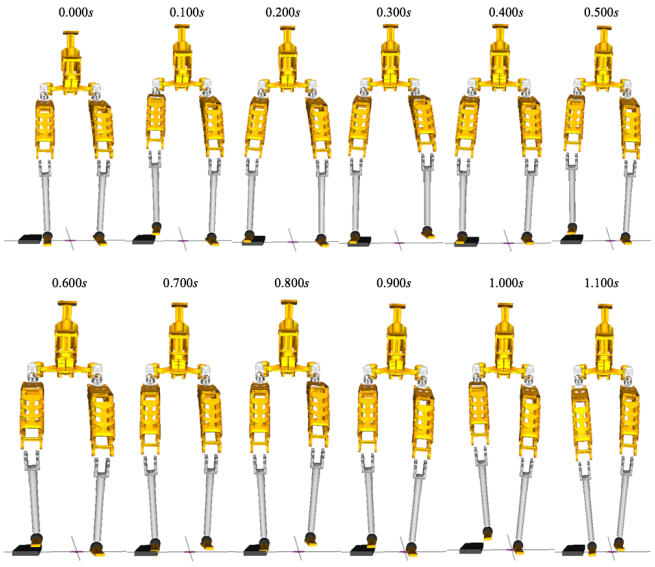

Fig. 9. Snapshots of stepping on unknown terrain. The black box is the obstacle. The robot does not have the prior knowledge about when to step on the obstacle. The time step of snapshots is 0.1 s

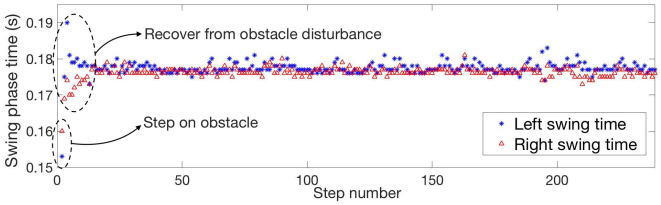

Fig. 10. Swing phase time is not constant but keeps changing with the unpredicted contact event during 239 steps' simulation. When the robot happens to step on the obstacle, the swing time is shortened because of landing head of time.

VI. CONCLUSIONS

In this study, WBOS framework is adopted for locomotion control. Compared with optimization-based inverse dynamics controller, WBOS framework is highly efficient in numerical computation. The CoM motion and the body posture are formulated as tasks in operational space. And all these tasks are glued together without task priority. The tasks are coupled naturally but simulation results show that the coupling effect is acceptable. A foot placement planner based on CoM position and velocity is embedded as tasks in WBOS framework. Since the dynamics model is switched based on contact events, a fixed swing time is not required. The simulation shows that the walking controller presents robustness to push recovery and unknown terrains. Sensing noises are also taken into account to demonstrate the practicability of the proposed controller.

One of the inherent properties of the biped robot is the floating base which could not provide control force to keep balance. For biped robot with foot and actuated ankle, the ground reaction force is unilateral and can not provide enough forces to prevent falling. Seeking a new foot placement is an option for recovering the balance. The limitation of foot placement recovery is its dependence on the reachable space determined by the kinematics configuration of the biped robot. Our future work includes deeper analysis of the robustness of controller framework proposed in this study and explore multiple-step recovery under larger push disturbances.

REFERENCES

[1] A.Hofmann. "Robust execution of bipedal walking tasks from biomechanical principles.".PhD thesis, MIT, Jan. 2006.

[2] Feng, Siyuan, et al. "Optimization based full body control for the atlas robot." Humanoid Robots (Humanoids), 2014 14th IEEE-RAS International Conference on. IEEE, 2014.

[3] Kajita, Shuuji, et al. "The 3D Linear Inverted Pendulum Mode: A simple modeling for a biped walking pattern generation." Intelligent Robots and Systems, 2001. Proceedings. 2001 IEEE/RSJ International Conference on. Vol. 1. IEEE, 2001.

[4] Kajita, Shuuji, et al. "A realtime pattern generator for biped walking." Robotics and Automation, 2002. Proceedings. ICRA'02. IEEE International Conference on. Vol. 1. IEEE, 2002.

[5] Kajita, Shuuji, et al. "Biped walking pattern generation by using preview control of zero-moment point." Robotics and Automation, 2003. Proceedings. ICRA'03. IEEE International Conference on. Vol. 2. IEEE, 2003.

[6] J. Pratt et al., Capturability-based analysis and control of legged locomo- tion, part 2: Application to m2v2, a lower body humanoid, Int. J. Robot. Res., vol. 31, no. 10, pp. 11171133, 2012.

[7] B. Stephens, Push recovery control for force-controlled humanoid robots, Ph.D. dissertation, , Carnegie Mellon Univ., Pittsburgh, PA, USA, 2011.
[8] Stephens, Benjamin J., and Christopher G. Atkeson. "Push recovery by stepping for humanoid robots with force controlled joints." Humanoid Robots (Humanoids), 2010 10th IEEE-RAS International Conference on. IEEE, 2010.
[9] Englsberger, Johannes, Christian Ott, and Alin Albu-Schffer. "Three-dimensional bipedal walking control based on divergent component of motion." IEEE Transactions on Robotics 31.2 (2015): 355-368.
[10] Hopkins, Michael A., Dennis W. Hong, and Alexander Leonessa. "Compliant locomotion using whole-body control and Divergent Component of Motion tracking." Robotics and Automation (ICRA), 2015 IEEE International Conference on. IEEE, 2015.
[11] Englsberger, Johannes, et al. "Trajectory generation for continuous leg forces during double support and heel-to-toe shift based on divergent component of motion." Intelligent Robots and Systems (IROS 2014), 2014 IEEE/RSJ International Conference on. IEEE, 2014.
[12] Geyer, Hartmut, Andre Seyfarth, and Reinhard Blickhan. "Compliant leg behaviour explains basic dynamics of walking and running." Proceedings of the Royal Society of London B: Biological Sciences 273.1603 (2006): 2861-2867.
[13] Vejdani, H. R., et al. "Bio-inspired swing leg control for spring-mass robots running on ground with unexpected height disturbance." Bioinspiration & biomimetics 8.4 (2013): 046006.
[14] A. Ramezani, J. W. Hurst, K. A. Hamed, and J. Grizzle, Performance analysis and feedback control of atrias, a 3D bipedal robot, Journal of Dynamic Systems, Measurement, and Control, 2013
[15] Rezazadeh, Siavash, et al. "Spring-mass walking with ATRIAS in 3D: Robust gait control spanning zero to 4.3 kph on a heavily underactuated bipedal robot." Proceedings of the ASME 2015 Dynamic Systems and Control Conference. 2015.
[16] Vejdani, H. R., et al. "Bio-inspired swing leg control for spring-mass robots running on ground with unexpected height disturbance." Bioinspiration & biomimetics 8.4 (2013): 046006.
[17] Kim, Donghyun, et al. "Stabilizing series-elastic point-foot bipeds using whole-body operational space control." IEEE Transactions on Robotics 32.6 (2016): 1362-1379.
[18] D. Kim, G. Thomas, and L. Sentis, Continuous cyclic stepping on 3D point-foot biped robots via constant time to velocity reversal, in Proc. IEEE Int. Conf. Control Autom. Robot. Vision, 2014, pp. 16371643.
[19] L. Sentis, Synthesis and control of whole-body behaviors in humanoid systems, Ph.D. dissertation, Stanford Univ., Stanford, CA, USA, 2007.
[20] Koolen, Twan, et al. "Design of a momentum-based control framework and application to the humanoid robot atlas." International Journal of Humanoid Robotics 13.01 (2016): 1650007.
[21] Pratt, Jerry, et al. Virtual model control: An intuitive approach for bipedal locomotion. The International Journal of Robotics Research 20.2 (2001): 129-143.
[22] Khatib, Oussama, and Burdick, Joel. Motion and force control of robot manipulators. Robotics and Automation. Proceedings. 1986 IEEE International Conference on. Vol. 3. IEEE, 1986a.
[23] Stephens, Benjamin J., and Atkeson, Christopher G..Dynamic balance force control for compliant humanoid robots. Intelligent Robots and Systems (IROS), 2010 IEEE/RSJ International Conference on. IEEE, 2010.
[24] Posa, Michael, Scott Kuindersma, and Russ Tedrake. "Optimization and stabilization of trajectories for constrained dynamical systems." Robotics and Automation (ICRA), 2016 IEEE International Conference on. IEEE, 2016.
[25] Feng, Siyuan, et al. "Optimizationbased Full Body Control for the DARPA Robotics Challenge." Journal of Field Robotics 32.2 (2015): 293-312.
[26] Righetti, Ludovic, and Schaal, Stefan. Quadratic programming for inverse dynamics with optimal distribution of contact forces. Humanoid Robots(Humanoids), 2012 12th IEEE-RAS International Conference on. IEEE, 2012.
[27] Johnson, Matthew, et al. Team IHMCs Lessons Learned from the DARPA Robotics Challenge Trials. Journal of Field Robotics 32.2 (2015): 192-208.
[28] Ott, Christian, Ranjan Mukherjee, and Yoshihiko Nakamura. "A hybrid system framework for unified impedance and admittance control." Journal of Intelligent & Robotic Systems 78.3-4 (2015): 359.
[29] M. Raibert, Legged Robots that Balance. MIT Press, Cambridge, MA.,1986.
[30] Yin, KangKang, Kevin Loken, and Michiel Van de Panne. "Simbicon: Simple biped locomotion control." ACM Transactions on Graphics (TOG). Vol. 26. No. 3. ACM, 2007.
[31] A. Goswami, Postural stability of biped robots and the footrotation indicator (FRI) point, International Journal of Robotics Research, vol. 18, no. 6, pp. 52333, Jun. 1999.
[32] Luo, Jian-wen, Yi-li Fu, and Shu-guo Wang. "3D stable biped walking control and implementation on real robot." Advanced Robotics (2017): 1-16.

View publication stats